

# Time–space Distribution Characteristics of the Circum-Pacific Seismic Belt Based on Multifractal Analysis

Linfeng Xu<sup>1</sup>, Jiemin Chen<sup>1</sup>, Zhixin Liu<sup>1,\*</sup>, Yan Liu<sup>2</sup> and Jiawei Tian<sup>2</sup>

<sup>1</sup>School of Life Science, Shaoxing University, Shaoxing 312000, Zhejiang, P. R. China

<sup>2</sup>School of Automation, University of Electronic Science <sup>3</sup>Technology of China, Chengdu 610054, Sichuan, P. R. China

**Abstract.** A complete scientific system of earthquake prediction has yet to be developed, and most studies on the time–space sequence of seismic activity analysis are based on existing seismic models. By applying fractal theory with the two aspects of magnitude and intensity, a new dimension is added. In this study, we applied multifractal theory to analyse data of the Circum-Pacific seismic belt, which contains multifractal spectrums such as the relation, relation, and relation. The results suggest that earthquakes in the area which we studied contain multifractal features. The study also shows that the time–space propagation characteristics of the earthquakes are affected by the internal geological structures of the region and the adjacent area.

## 1 Introduction

Earthquakes seriously endanger human safety and property safety and cause great loss to society [1]. Limitations and constraints exist in people’s understanding of earthquakes [2]. Many factors cause difficulties in achieving research breakthroughs on seismic activity and the worldwide acceptance of seismic prediction problems [3-5].

This study focuses on the earthquakes in the Circum-Pacific seismic belt occurred between 1900 and 2015 and explores the time–space characteristics of their seismic activities [6-9]. Data is obtained from the database of the US Geological Survey (USGS). Fractal theory [10] is used to analyze the characteristics of the time–space distribution by nonlinear analysis [11]. Finally, this paper identifies causal relationships among the characteristics of the time–space distribution and of the geological structures.

Fractal theory has been used to study seismic time–space distribution characteristics since many years ago [12-18]. In 1986, Kawakatsu [19] identified different levels of contrast, intermittent, periodicity, rarefaction and congestion among singular spectrums and fractal dimensions in different seismic zones by analyzing the seismic data in the Tianshan-Pamir, Caucasus, and California zones, and these are important characteristics in seismic prediction. Geilikman et al. [20] used multifractal characteristics which were calculated in three different regions, which contain information about spatial earthquake

---

\*Corresponding author: [liuzhixin@usx.edu.cn](mailto:liuzhixin@usx.edu.cn)

distribution. In 1988, Kagan and Kuopoff [21] used fractal theory in the study of the space distribution features and demonstrated [5] that scale-invariance and fractal structures exist in the time–space sequences. In 2003, David Harte [22] stated that the Hill multifractal method can be applied to study seismic generalized strain energy. After comparing the characteristics of earthquakes in different regions, he found that strong relationships exist among the fractal characteristics of the seismic energy and the complexity of geological structures. In 2011, Roy and Mondal [23] introduced the multifractal method to analyze the variation sequences in seismic electromagnetic flow. They concluded that an outlier existed in the dimension of the electromagnetic flow before a strong earthquake. Balcerak [24] performed a study based on the Tokachi-oki earthquake and determined that an outlier exists in the multifractal dimension of seismic activity before the next earthquake based on the seismic sequences. Using wavelet analysis, Li X., Zheng W., et. al. studied the seismic data in southwest occurred between 1900 and 2013 [25]. In 2003, Pisarenko and Sornette applied the GPD approach and proposed a physical mechanism contrasting “crack-type” rupture with “dislocation-type” behavior[26]. And about fifteen years later, Pisarenko and others then found the duality between the GEV and GPD, which means that a new way appeared to check the consistency of the estimation of the tail characteristics of distribution of earthquake magnitudes for earthquake occurring over an arbitrary time interval [26].

Multifractal theory is the pointcut in our research on the characteristics of the time–space distribution in seismic activities [27]. We depicted the factor of the fractal spectrum and comprehensively analyze the time–space characteristics of the geological structures.

## **2 Study area and data description**

### **2.1 Overview of the research area**

The Circum-Pacific seismic belt comprises adjacent areas in the center of the Pacific. Given that the Circum-Pacific belt is the largest and the most active seismic belt in the world, the earthquakes in this belt account for 80% of earthquakes in the world. Most are shallow quakes with high frequency, which will be a significant threat to the seismic zone and its adjacent areas [28]. The regularity of the earthquakes will therefore be determined in this study by analyzing the time–space distribution characteristics of data on the seismic activity in the Circum-Pacific seismic zone.

### **2.2 Data sources**

The seismic data in this paper come from the official website of the United States Geological Survey, which aims to provide policy makers and the public with extensive, high-quality and timely scientific information [29]. The region of the data ranges from 70°N to 50°S, with its longitude ranging from 100°E to 50°W. The minimum magnitude of an earthquake is -2 or even smaller, which is the initial reference. An integrity analysis of the data shows that the minimum earthquake magnitude is 4.4. Thus, we select the seismic data with  $M_s \geq 4.4$  as the research sample of this study.

### 3 Method and processing

#### 3.1 Multifractal analysis

A multi-fractal object is more complicated than fractal object, because it is always invariant by translation, where the dilatation factor is needed to differentiate the detail from all the object [30-36].

The form of multi-fractal is defined by:

$$D(H) = \inf_q (q * h - \tau(q) + c) \tag{1}$$

where  $q$  is a real,  $c$  is constant and  $\tau(q)$  is called the partition function.

The parameter  $q$  represents a microscope for exploring different regions of the singular measurement. If  $q$  is higher than 1,  $D_q$  represents strange regions, and else if  $q$  is lower than 1,  $D_q$  accentuates not so strange regions, and if  $q$  equals 1,  $D_q$  means the information dimension [37].

Consider Hölder exponents  $h$  of particles whose values between  $[h, h+\Delta h]$ , which consist the set  $E(h)$ ,  $f(h)$  is the definition as the FD of this set, that has a single fractal structure. Link the pairs  $(q, \tau(q))$  and  $(h, f(h))$  with the Legendre transform [37]:

$$\begin{aligned} \tau(q) &= q * h(q) - f(q) \\ h(q) &\cong \alpha(q) = \frac{d\tau(q)}{dq} \end{aligned} \tag{2}$$

where  $\alpha$  is an approximation of  $h$ .

To a multi-fractal object,  $D_q$  is a decreasing function, and  $f(h)$  is convex which means its maximum equals the Hausdorff dimension  $D_h$ .

### 4 Results

#### 4.1 Multifractal analysis of the time-space sequence of the research zone

We can depict the intensity of earthquakes in the zone of study, and the energy of the seismic activity can show the transferability of the earthquakes [38]. Therefore, this paper will focus on the multifractal spectrum analysis of time-space distribution characteristics by studying seismic energy, which will provide some information on the time-space characteristics of seismic activity [39,40].

The  $\ln \varepsilon - \ln X_q$  diagram within the different weighting factors of the earthquakes in the target zones can be drawn based on multifractal theory (Figure 1). The time-series diagram of the energy released in the earthquake shown in figure 1(a) indicates that a good linear relation between  $\ln X_q$  and  $\ln \varepsilon$  is presented within the region of the weighting factor  $q$ . But their slopes show a difference within various factors. Furthermore, the curves are divergent when  $\varepsilon \rightarrow -\infty$  but convergent when  $\varepsilon \rightarrow +\infty$ , which suggests that a significant scale invariance can show the time sequence of the earthquakes in the research zone and that its multifractal property of the time series also can be depicted.

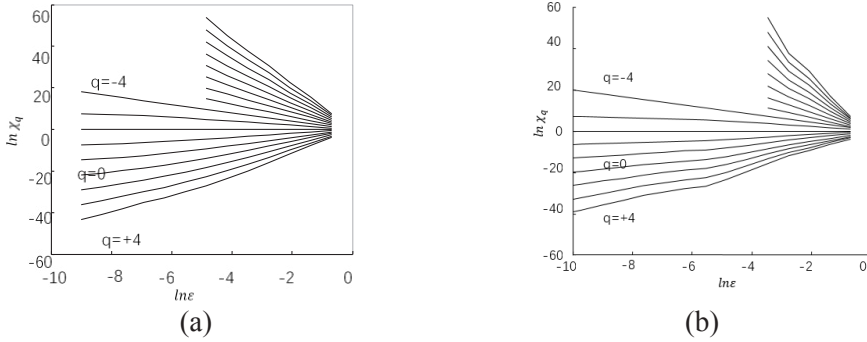


**Fig. 1.**  $\ln \varepsilon - \ln X_q$  diagram of the Circum-Pacific seismic belt (a) Time series (b) Spatial sequence

Based on the figure of  $\ln \varepsilon - \ln X_q$ , the multifractal characteristics of the earthquakes in the research zone are represented by fitting the corresponding segments of the value of the weighting factor  $q$  to acquire the quality index  $\tau(q)$  by a single variable linear regression. The slope of the whole curve can be divided into three parts according to figure 2(a). The middle part possesses the largest slope, and a significant difference is seen between the first and last parts. These features show the impressive multifractal property of the earthquake energy of the time series and also suggest that the middle part of the time series has the largest multifractal property [5].

The degree of the multifractal spectrum characteristic of the seismic activity is measured by the quality function  $\tau(q)$ . For a comprehensive description of the intensity of the multifractal time series, the multifractal characteristic can also be illustrated with respect to the dimension of information and the singular spectrum based on multifractal theory.

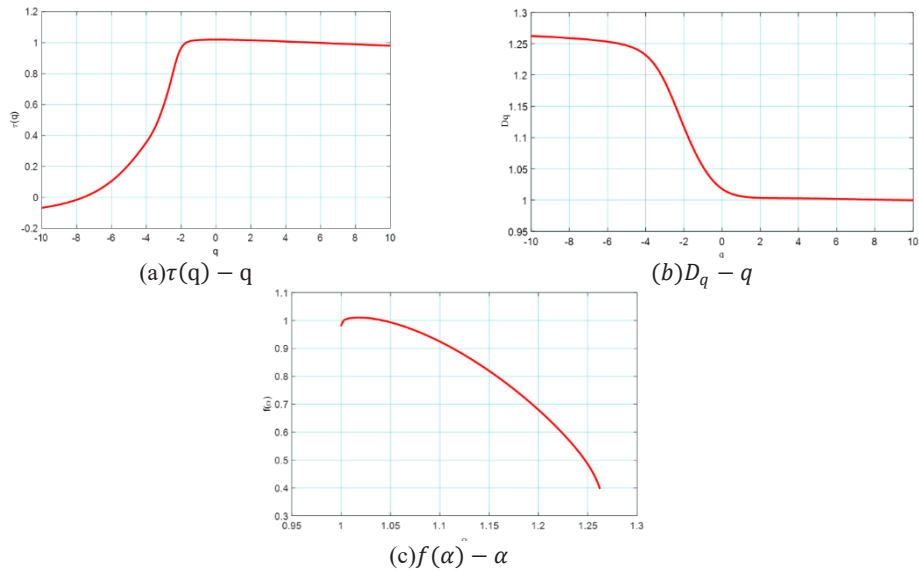


**Fig.2.** Diagrams of time series of the study belt

As for the dimension of information,  $D_q$  is a nonlinear decreasing function, which decreases as  $q$  increases. The value of  $q$  corresponds to a specific value of  $D_q$ , which depicts the quiet and the active period of the earthquake in the seismic belt. The reason for the less

obvious seismic activity in time series calculated  $D_q - q$  curve is that highlighting the singularity in the local scale out of the complexity is difficult. As a whole, the seismic activity initially decreases rapidly (Figure 2(b)) before increasing slowly with  $D_0 = 0.56$ . The reason for this occurrence may be associated with the uneven distribution of the seismic energy in each region attributed to the various stresses. Thus, a highly complex multifunction of the earthquake in the seismic belt and seismic activity is suggested.

Figure 2(c) shows the singular spectrum of the time series. The asymmetry, continuity, and smoothness are shown in the time sequence curve  $f(\alpha) - \alpha$  of the earthquakes happened in the seismic belt. The vertex of the earthquake is located at the center-left, which conforms to the characteristics of the sparse multifunction. The left part of the whole curve depicts the sparseness of the earthquake, and the right part shows the clustering. The non-convergence of the left part of the curve suggests that the tensity distribution in the time series of the earthquake only clusters with illimitability and less sparsity. The immense difference between the two parts of the curve signifies a difference in the sharpness of the singular spectrum of time inconsistency, which suggests the presence of a small  $\alpha_{min}$  and a similarity in the clustering of the seismic tensity of time inconsistency.

### 4.2 Multifractal analysis of the time series in the research zone

The integrity of the time series of the earthquakes is shown with the discretization of the earthquakes in the seismic belt at different resolutions. The integrity divides the seismic data into different grids according to some standards (Figure 3). The earthquakes energy in every grid will be used in statistical analysis to generate a 2D field of the seismic energy. The result can be shown as follows:

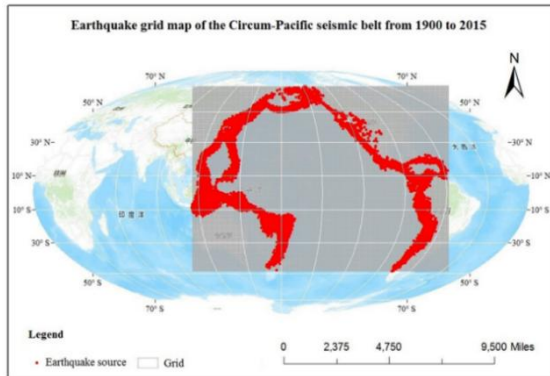


**Fig. 3.** Earthquake grid map of the study area

In general, immense differences exist among the seismic energy values within the changes of space in the seismic belt. The  $\ln \varepsilon - \ln X_q$  curve in the space distribution sequence can be drawn and compared with the multifractal analysis of the time sequence (Figure 1(b)). A good linear relationship between  $\ln X_q$  and  $\ln \varepsilon$  is more variable than the time sequence is suggested. This relationship signifies that the scale invariance, the multifractal complexity, and the multifractal property of the seismic zone are more noticeable in the space series than in the time series.

Compared with the multifractal analysis in the time sequence, as shown in figure4(b), the slope of the  $\tau(q) - q$  curve changes continuously, initially increasing before decreasing. This pattern suggests the existence of the multifractal property of the seismic energy in the space series. The difference between the two stages and the nonlinearity are

clearly shown, thereby suggesting a more complex and more multifractal property in the seismic space series than in the seismic time series.

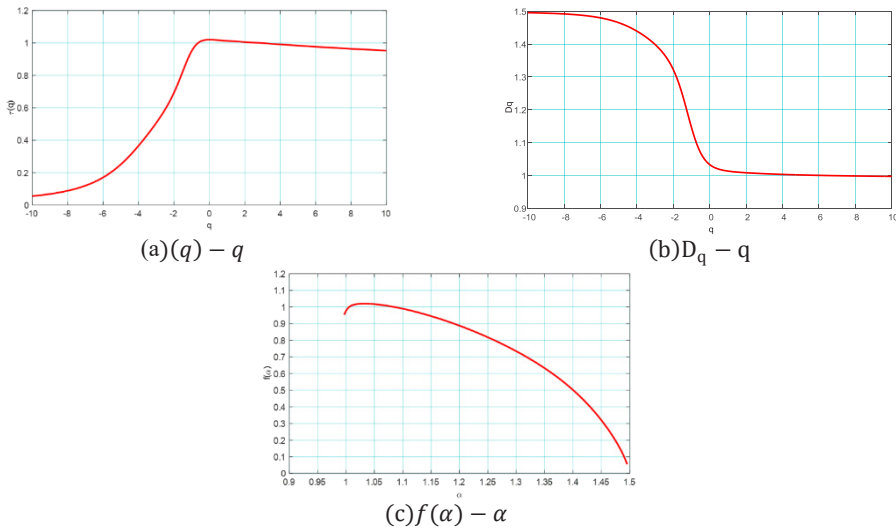


**Fig. 4.** Diagrams of spatial sequence of the Circum-Pacific seismic belt

For the information dimension,  $D_q - q$ , the spectrum of the information dimension in the space distribution series can be accomplished by using the multifractal theory. The complexity of the multifractal is depicted in figure 6(b), which indicates that it is compliance with the intricacy of the geological structure.

The diagram  $f(\alpha) - \alpha$  (Figure 4(c)), which is used for the analysis of the seismic space series, is the curve with asymmetry, continuity, and smoothness. The proportion of the unit with the maximum and minimum probability can be obtained through the value of  $\Delta f$ , which illustrates the characteristics of the earthquakes in the space sequence by describing the seismic energy in the peak and the trough.  $f(\alpha_{min}) = 1.15$  and  $f(\alpha_{max}) = 1.15$  coincide with  $\Delta f = 0.40$ , thereby indicating that the left of the peak is hooked and that the multifractal property is sparse. The curve is skewed to the right within the region of  $\alpha$ , which signifies a large percentage of the seismic clustering and a higher frequency of seismic energy in the clustering earthquakes than in the sparse earthquakes. Thus, the clustering in the seismic time sequence is the main characteristic of the seismic activity.

## 5 Discussion and conclusions

Based on multifractal theory, this paper aims at the acquisition and analysis about the multifractal spectrum of earthquake activities that occurred in the Circum-Pacific seismic zone in time and space sequences. The results indicate the following:

The theoretical value of the weighting factor  $q$  is the whole set of real numbers, where a larger value has a better implication, thereby illustrating the changing conditions of the fractal dimension of the research objects. In reality, considering the amount of computation and the final result, the region of  $q$  can neither be excessively large nor small which may cause the loss of an essential message because of the incomplete multifractal spectrum or the large fluctuating range of the multifractal spectrum. Thus, compared with the empirical value, the final region of  $q$  is defined as  $[-10,10]$  after conducting several experiments based on the seismic data within integrity processing.

The  $\ln \varepsilon - \ln X_q$  diagram, which depicts the time sequence of the earthquakes in the research area, shows that a multifractal structure exists in the time series of the seismic belt. The curve depicts a strong linear relationship within the region of  $q$ , which can extend to infinity with a small  $\varepsilon$  value. This relationship shows the ideal scale invariance and the evident multifractal property in the time sequence. The curve can be divided into two parts in the inflection point with a different slope. The probability of the seismic data becomes small in the box when the region of the box is sufficiently small, thus indicating that not all the  $\varepsilon$  values can satisfy the scale invariance. The reason for the bad linear relationship within the positive weighting factor is that less consideration in the lower bound of  $\varepsilon$  is given when dividing the data into the grids. Insufficient consideration weakens the linear relation because of the lack of samples. This result also induces an incomplete multifractal property and the fluctuation of the log-log diagram.

The variety of the quality index in the seismic time series shows the multifractal property and strength the phase of the energy released in the earthquakes. The nonlinearity of the quality index is strong, and the slope of different weighting factors shows the difference. This result signifies the immense multifractal property of the seismic energy and the existence of the strength phase of the multifractal property of the earthquake in the time sequence.

The dimension of the information in the seismic time series illustrates that the complexity of the earthquakes and its multifractal.  $D_q$  is the decreased nonlinear function, which represents the quiet period. The active period, clustering, and sparseness are corresponded with different  $q$  values. As a whole, the seismic activity initially decreased rapidly in the figure  $D_q - q$  and later increased slowly with  $D_0 = 0.56$ . The reason for this pattern may be associated with the uneven distribution of the seismic energy in each region attributed to various stresses, thereby showing the compliance of seismic energy with the complexity of the geological structure.

The multifractal spectrum  $f(\alpha)$  of the earthquake in a time series involves the asymmetric, continuous, and sparse curve with a significant difference between the two parts of the  $f(\alpha) - \alpha$  curve and a small value of  $\alpha_{\min}$ . These attributes show the similarity.  $\Delta\alpha = 0.37$ , and  $\Delta f = 0.555$ . These values show that the vertex is of the center-left, which conforms to the characteristic of the sparse multifunction. The left part of the spectrum shows the sparse features of the earthquake, whereas the right part shows the clustering characteristics. The infinite nature of the sparse features indicates the absence of a specific value of  $\alpha$  in the left part, thereby suggesting that the tensivity distribution in time series of the earthquake only possesses clustering with illimitability but with less sparsity.

In conclusion, this paper applies fractal theory and performs a multifractal analysis of earthquakes and seismic energy. The result clarifies the characteristics of the seismic activity and uncovers strong relationships among time-space propagation characteristics and geological structures in the target and adjacent areas.

## 6 Acknowledgments

This work was jointly supported by the National College Students Innovation and Entrepreneurship Training Program (No.201910349017&No.202010349024)

## References

- [1] X Li, N Lam, Y Qiang, K Li, L Yin, S Liu, W Zheng, Measuring county resilience after the 2008 Wenchuan earthquake, *International Journal of Disaster Risk Science* 7 (4), 393-412.
- [2] Zheng, W., Li, X., Yin, L., Yin, Z., Yang, B., Liu, S., ... & Li, Y. (2017). Wavelet analysis of the temporal-spatial distribution in the Eurasia seismic belt. *International Journal of Wavelets, Multiresolution and Information Processing*, 15(03), 1750018.
- [3] Liu, S., Gao, Y., Zheng, W., & Li, X. (2015). Performance of two neural network models in bathymetry. *Remote sensing letters*, 6(4), 321-330.
- [4] Zheng, W., Li, X., Lam, N., Wang, X., Liu, S., Yu, X., ... & Yao, J. (2013). Applications of integrated geophysical method in archaeological surveys of the ancient Shu ruins. *Journal of archaeological science*, 40(1), 166-175.
- [5] Yin, L., Li, X., Zheng, W., Yin, Z., Song, L., Ge, L., & Zeng, Q. (2019). Fractal dimension analysis for seismicity spatial and temporal distribution in the circum-Pacific seismic belt. *Journal of Earth System Science*, 128(1), 22.
- [6] Zheng, W., Li, X., Xie, J., Yin, L., & Wang, Y. (2015). Impact of human activities on haze in Beijing based on grey relational analysis. *Rendiconti Lincei*, 26(2), 187-192.
- [7] Xu, C., Yang, B., Guo, F., Zheng, W., & Pognet, P. (2020). Sparse-view CBCT reconstruction via weighted Schatten p-norm minimization. *Optics Express*, 28(24), 35469-35482.
- [8] Liu, S., Zhang, Y., Zheng, W., & Yang, B. (2019, February). Real-time Simulation of Virtual Palpation System. In *IOP Conference Series: Earth and Environmental Science* (Vol. 234, No. 1, p. 012070). IOP Publishing.
- [9] Dankwa, S., & Zheng, W. (2019). Special Issue on Using Machine Learning Algorithms in the Prediction of Kyphosis Disease: A Comparative Study. *Applied Sciences*, 9(16), 3322.
- [10] Li, X., Zheng, W., Wang, D., Yin, L., & Wang, Y. (2015). Predicting seismicity trend in southwest of China based on wavelet analysis. *International Journal of Wavelets, Multiresolution and Information Processing*, 13(02), 1550011.
- [11] Chen, X., Yin, L., Fan, Y., Song, L., Ji, T., Liu, Y., ... & Zheng, W. (2019). Temporal evolution characteristics of PM<sub>2.5</sub> concentration based on continuous wavelet transform. *Science of The Total Environment*, 134244.
- [12] Li X., Yin L., Yao L., Yu W., She X., Wei W. (2020). Seismic spatiotemporal characteristics in the Alpid Himalayan Seismic Belt, *Earth Science Informatics*, 13, 883–892.
- [13] Yang, B., Liu, C., Zheng, W., Liu, S., & Huang, K. (2018). Reconstructing a 3D heart surface with stereo-endoscope by learning eigen-shapes, *Biomedical optics express* 9 (12), 6222-6236
- [14] Liu, S., Zheng, W., & Yang, B. (2018, August). Adaptive Terminal Sliding Mode Control for Time-delay Teleoperation with Uncertainties. In *2018 IEEE International Conference on Mechatronics and Automation (ICMA)* (pp. 1883-1888). IEEE.
- [15] Dankwa, S., Zheng, W., Gao, B., & Li, X. (2018, July). Terrestrial Water Storage (TWS) Patterns Monitoring in the Amazon Basin Using Grace Observed: its Trends and Characteristics. In *IGARSS 2018-2018 IEEE International Geoscience and Remote Sensing Symposium* (pp. 768-771). IEEE.



- [16] Yang, B., Cao, T., Zheng, W., & Liu, S. (2018, July). Motion Tracking for Beating Heart Based on Sparse Statistic Pose Modeling. *In 2018 40th Annual International Conference of the IEEE Engineering in Medicine and Biology Society (EMBC) (pp. 1106-1110)*. IEEE.
- [17] Liu, H., Su, H., Li, X., & Zheng, W. (2018). Deriving bathymetry from optical images with a localized neural network algorithm. *IEEE Transactions on Geoscience and Remote Sensing*, 56(9), 5334-5342.
- [18] Liu, S., Zhang, X., Zheng, W., & Yang, B. (2017, December). Adaptive neural network control for time-delay teleoperation with uncertainties. *In 2017 11th Asian Control Conference (ASCC) (pp. 1270-1275)*. IEEE.
- [19] Tang, Y., Liu, S., Li, X., Fan, Y., Deng, Y., Liu, Y., & Yin, L. (2020). Earthquakes spatio-temporal distribution and fractal analysis in the Eurasian seismic belt. *Rendiconti Lincei. Scienze Fisiche e Naturali*, 31(1), 203-209.
- [20] Ma, Z., Zheng, W., Chen, X., & Yin, L. (2021). Joint embedding VQA model based on dynamic word vector. *PeerJ Computer Science*, 7, e353.
- [21] Zheng, W., Liu, X., & Yin, L. (2021). Sentence Representation Method Based on Multi-Layer Semantic Network. *Applied Sciences*, 11(3), 1316.
- [22] Tang Y., Liu S., Deng Y., Zhang Y., Yin L., Zheng W. (2021), An improved method for soft tissue modelling, *Biomedical Signal Processing and Control*, 65, 102367
- [23] Wang, B., Wu, W., Zheng, W., Liu, Y., & Yin, L. (2020, November). Recommendation Algorithm of Crowdfunding Platform Based on Collaborative Filtering. *In Journal of Physics: Conference Series (Vol. 1673, No. 1, p. 012030)*. IOP Publishing.
- [24] Wu, W., Wang, B., Zheng, W., Liu, Y., & Yin, L. (2020, November). Higher Education Online Courses Personalized Recommendation Algorithm Based on Score and Attributes. *In Journal of Physics: Conference Series (Vol. 1673, No. 1, p. 012025)*. IOP Publishing.
- [25] Tang, Y., Liu, S., Deng, Y., Zhang, Y., Yin, L., & Zheng, W. (2020). Construction of force haptic reappearance system based on Geomagic Touch haptic device. *Computer methods and programs in biomedicine*, 190, 105344.
- [26] Pisarenko, V. F., & Sornette, D.. (2003). Characterization of the frequency of extreme events by the generalized pareto distribution. *Pure & Applied Geophysics*, 160(12), 2343-2364.
- [27] Ni, X., Yin, L., Chen, X., Liu, S., Yang, B., & Zheng, W. (2019). Semantic representation for visual reasoning. *In MATEC Web of Conferences (Vol. 277, p. 02006)*. EDP Sciences.
- [28] Li, X., Zheng, W., Yin, L., Yin, Z., Song, L., & Tian, X. (2017). Influence of social-economic activities on air pollutants in Beijing, China. *Open Geosciences*, 9(1), 314-321.
- [29] USGS. <http://earthquake.usgs.gov/earthquakes/search/>.
- [30] Yang, B., Liu, C., Huang, K., & Zheng, W. (2017). A triangular radial cubic spline deformation model for efficient 3D beating heart tracking. *Signal, Image and Video Processing*, 11(7), 1329-1336.
- [31] Huang, W., Zheng, W., & Mo, L. (2017). Distributed robust  $H_\infty$  composite-rotating consensus of second-order multi-agent systems. *International Journal of Distributed Sensor Networks*, 13(7), 1550147717722513.

- [32] Yang, B., Liu, C., Zheng, W., & Liu, S. (2017). Motion prediction via online instantaneous frequency estimation for vision-based beating heart tracking. *Information Fusion*, 35, 58-67.
- [33] Zhou, Y., Zheng, W., & Shen, Z. (2016). A New Algorithm for Distributed Control Problem with Shortest-Distance Constraints. *Mathematical Problems in Engineering*, 2016.
- [34] Li, X., Zheng, W., Lam, N., Wang, D., Yin, L., & Yin, Z. (2017). Impact of land use on urban water-logging disaster: a case study of Beijing and New York cities. *Environmental Engineering & Management Journal (EEMJ)*, 16(5).
- [35] Xun, L., & Wenfeng, Z. (2013, June). Parallel spatial index algorithm based on Hilbert partition. In *2013 International Conference on Computational and Information Sciences* (pp. 876-879). IEEE.
- [36] Zheng, W., Liu, X., Ni, X., Yin, L., & Yang, B. (2021). Improving Visual Reasoning through Semantic Representation. *IEEE Access*.
- [37] Lopes, R., & Betrouni, N. (2009). Fractal and multifractal analysis: a review. *Medical Image Analysis*, 13(4), 634-649.
- [38] Zheng, W., Li, X., Yin, L., & Wang, Y. (2016). The retrieved urban LST in Beijing based on TM, HJ-1B and MODIS. *Arabian Journal for Science and Engineering*, 41(6), 2325-2332.
- [39] Zheng, W., Li, X., Yin, L., & Wang, Y. (2016). Spatiotemporal heterogeneity of urban air pollution in China based on spatial analysis. *Rendiconti Lincei*, 27(2), 351-356.
- [40] Ding, Y., Tian, X., Yin, L., Chen, X., Liu, S., Yang, B., & Zheng, W. (2019, September). Multi-scale Relation Network for Few-Shot Learning Based on Meta-learning. In *International Conference on Computer Vision Systems* (pp. 343-352). Springer, Cham.